P1.10 BOUNDARY LAYER OBSERVATIONS OF COLD AIR POOLS IN A MOUNTAIN BASIN

E. G. Astling*, C. A. Biltoft, D. Storwold,
Meteorology & Obscurants Division, West Desert Test Center
Dugway, UT 84022
and
S. A. McLaughlin
NOAA Environmental Technology Laboratory
Boulder, CO 80303

1. INTRODUCTION

Cold air pools are frequently observed in topographically confined areas throughout the western United States. These surface-based stable layers appear in mountain basins ranging in size from 1^2 to 10^5 km (Whiteman et al. 2001; Clements et al. 2000). These features may persist for several days in the wintertime and develop in nighttime hours during other times of the year when no synoptic-scale transient systems are present. Dispersion of atmospheric pollutants in cold air pools is often a problem because of their stable stratification and relatively weak wind fields. Formation and intensity of cold pools is a challenging forecast problems in basin and valley regions (Smith et al. 1997).

In this paper, we investigate the evolution of cold pools that form in the Great Salt Lake Desert. The cold air pools are frequently observed in this region from a Surface Atmospheric Measurement System (SAMS) with measurement sites located at mountain-basin and ridge-top locations. The study focuses on a 5-day period during a special field program in September 2001 at the West Desert Test Center when SAMS and 924-MHz profiler data were enhanced with other data including measurements from a frequency-modulated continuous-wave (FM-CW) radar (McLaughlin and Eaton 1993). During this period, well-defined diurnal cold pools were observed with multiple stratified layers and complex wave structure.

*Corresponding author address: Elford G. Astling, West Desert Test Center, U.S. Army Dugway Proving Ground, UT 84022 astling@dpg.army.mil

2. TOPOGRAPHIC FEATURES

The Great Salt Lake Desert, one of the major mountain basins in the western United States, covers an area of about 24,000 km^2 in northwestern Utah. The arid region is a closed basin that is relatively flat and surrounded by mountains with peaks extending 1 to 2 km above the basin floor. The study area was located in the basin's southeastern corner where fine silty clay soils and sparse desert shrubs cover the landscape. These topographic features and land-surface characteristics provide favorable conditions for cold air pool development (Whiteman 2001).

3. MEASUREMENT SYSTEMS

Figure 1 shows a number of instruments that were deployed in the desert basin to provide high-resolution temporal and spatial data during the evolution of cold

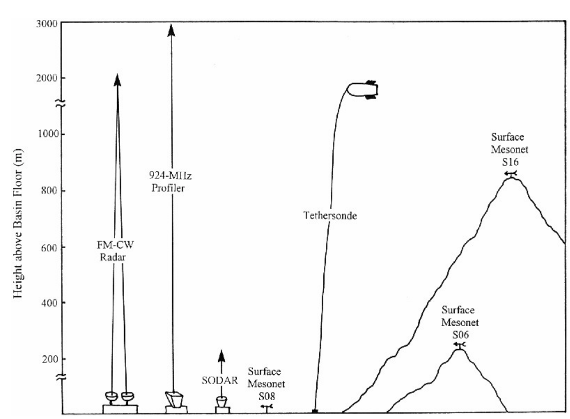

Figure 1. Schematic representation of the instrumentation with respect to elevation above the desert-basin floor.

air pool events. Measurements were provided at various levels from the basin floor to heights up to 3000 m. Fifteen-minute averages of air temperature, wind, and pressure were obtained at three SAMS sites. S8 was located in the mountain basin. S6 and S16 were located on mountain ridge tops at 274 m and 839 m above the basin floor, respectively. The 924-MHz profiler was co-located with S8 and provided 30-min consensus averages of boundary-layer winds at a 60-m resolution between 120 and 3000 m AGL. Three portable instruments were operated at the S8 site. A frequency modulated-continuous wave (FM-CW) radar was used to profile the refractive-index structure parameter (C_n^2) with a temporal resolution of 8 seconds and a spatial resolution on the order of 1 m. A sound direction and ranging (SODAR) system was used to measure vertical profiles of wind and turbulence. The SODAR provided 15-min averaged wind profiles between 15 and 200 m AGL in 5-m intervals (Metzger et al. 2001). A number of tethersonde flights were conducted at specific times to obtain wind and thermodynamic profiles between the surface and approximately 1500 m AGL.

4. OBSERVATIONS OF DIURNAL COLD POOLS

Figure 2 shows the evolution of diurnal cold pools at the West Desert Test Center for the period 21-25 September 2001. The time series of surface temperature shows that diurnal temperature ranges were on the order of 30° C for the mountain basin site (S8) and only 10° C for the mountain top site (S16). Stratified layers developed near 2100 LST and intensified until sunrise with mountain-top temperatures 5° to 10° C warmer than at the mountain-basin floor. It should be noted that nocturnal temperature fluctuations were more pronounced at S8 than at S16. Also, timing of the inversion dissipation after sunrise was more irregular than the timing of its onset. Nighttime surface temperatures at other sites in the Great Salt Lake Desert were also colder than the temperatures at S16 and suggest that the diurnal cold pool extended throughout the desert basin during this period.

Wind directions were highly variable and tended to back with height on nights when the cold pool was strongest and the ridge-top wind speeds were less than 10 mph. The flow direction was generally easterly and southerly at S16 except in the early afternoon hours on 21 and 22 Sep when the flow direction was northwesterly. The afternoon northwesterly flow may be associated with a mountain-basin circulation (Rife et al. 2002). The 924-MHz profiler data (not shown) indicate that westerly and southwesterly flow prevailed above the mountain-tops, and no strong synoptic-scale weather events occurred during this period. National Weather Service radiosonde data from Salt Lake City and other nearby upper-air stations show that the atmospheric circulation over the region was characterized by anticyclonic flow and subsidence at the 500-hPa level.

Diagnosis of the inversion structure evolution was carried out by computing the Froude number from the time series of SAMS measurements at S8 and S16. As discussed by Smith (1989), the Froude number is useful in determining whether air flow will ascend over mountain barriers or be blocked or trapped in the case of cold air pools. The Froude number is a function of wind speed and atmospheric stability and is defined as:

$$Fr = U/NH \qquad (1)$$

Where U is the upstream wind speed, N is the Brunt-Vaisala frequency, and H is the height of the mountain top. The Brunt-Vaisala frequency is given by

$$N^2 = g/\theta \cdot \partial\theta/\partial z \qquad (2)$$

where g is the gravitational acceleration and θ is potential temperature. An average mountain top height of 800 m was used to represent H for the mountains surrounding the Great Salt Lake Desert and wind speeds

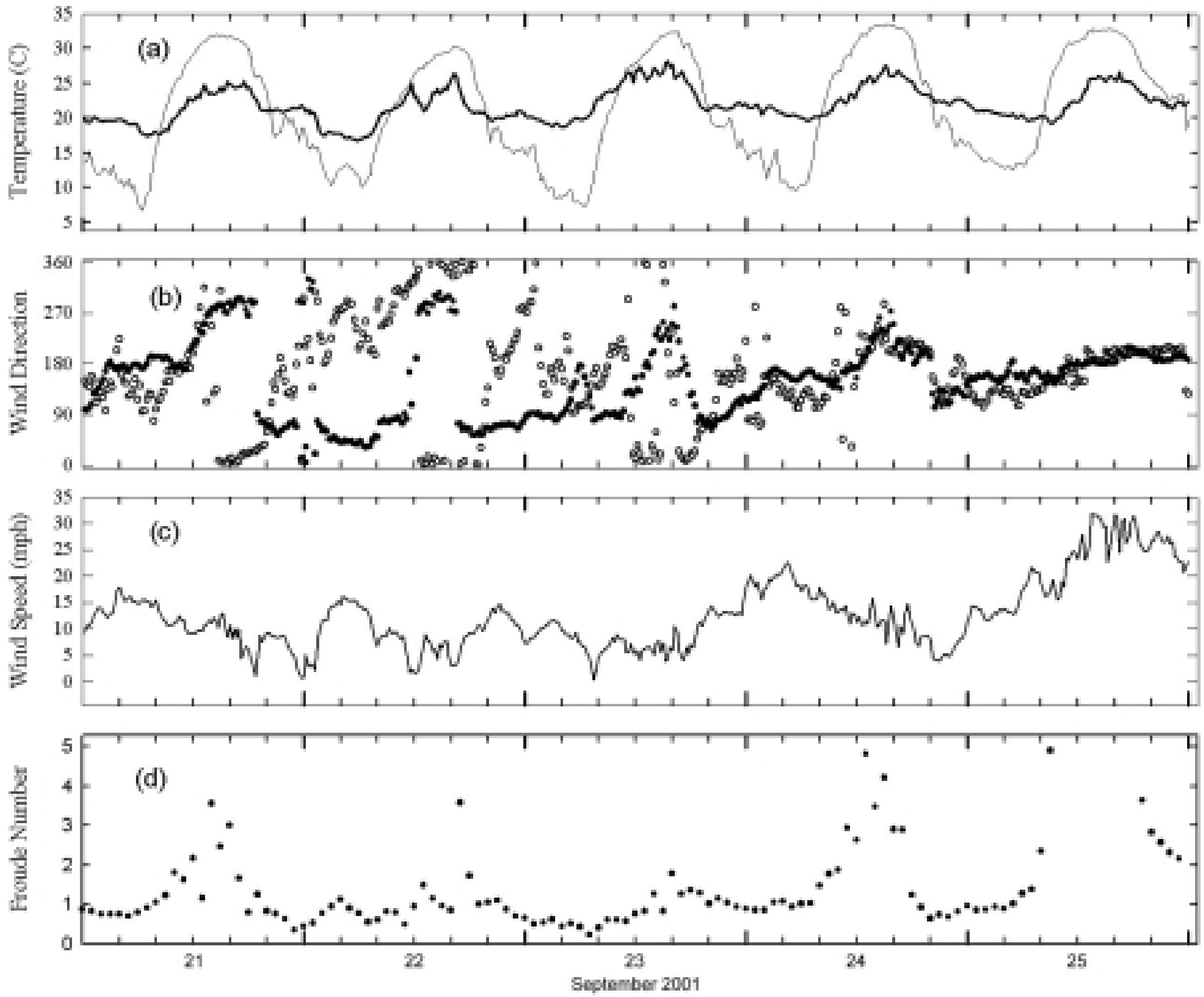

Figure 2. Time series of SAMS measurements of (a) surface temperature at S8 (light line) and S16 (heavy line), (b) wind direction at S8 (open circles) and S16 (solid circles), (c) wind speed at S16, and (d) Froude number.

measured at S16 were used for *U*. Because horizontal temperature gradients between stations at a given elevation are considerably less than vertical temperature gradients at different elevations in the western United States, as shown by Horel et al. (2002), $\partial\theta/\partial z$ in Eq. 2 was obtained with measurements from S8 and S16.

Figure 2d shows the time series of hourly averaged Froude numbers for the 5-day period. *Fr* values were less than 1.0 during the diurnal cold pool events and were less than 0.5 on 23 Sep when the inversion was strongest. Low Froude number flow persisted into the early morning hours on days when multiple stratified layers appeared in FM-CW radar images.

Figure 3 shows a 2-hr time-height display of FM-CW radar backscatter of clear-air structures from 0400 to 0559 LST on 23 Sep when the diurnal cold air pool was the strongest. The radar backscatter in these image profiles for clear air conditions are generally attributed to scattering by temperature and moisture gradients and by point targets such as insects and birds which may act as tracers. Turbulence creates spatial and temporal variations in the clear-air refractive index and produces scattering of electromagnetic waves. Multiple stratified layers and

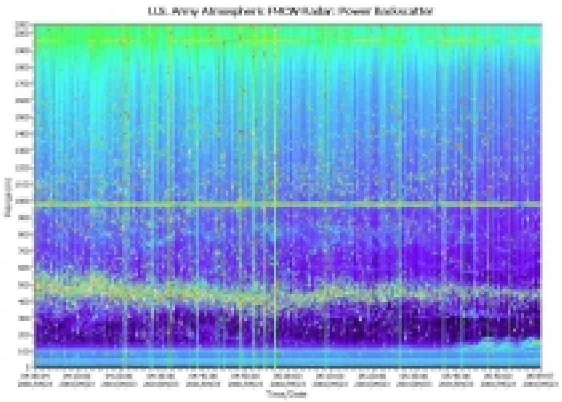

Figure 3. Time-height display of FM-CW radar backscatter during a 2-hr period on 23 Sep 2001.

complex wave patterns appear in this and many other profiles obtained during the 5-day period.

Two stratified layers are evident in Figure 3. A distinct bright-band feature is obvious in the 400-500 m layer during this 2-h period. The speckled appearance and lack of sharp gradients in the backscatter signal suggests that radar returns were from insects and were likely clustered within the most stable portion of the inversion. The inversion depth was typical of the nocturnal boundary layer structure for this region (Astling 1998). A second stratified feature was detected near 100 m with somewhat weaker radar returns. This feature evolved into wave structures and developed up to 160 m during the last 10 min. The FM-CW data detected turbulence associated with gravity and Kelvin-Helmholtz waves during cold-air pool events on other nights. Daytime breakup of the cold pool appeared to be related to convective plume development during daytime surface heating rather than to synoptic-scale forcing.

6. SUMMARY

Time series measurements from ground-based instruments and very high resolution radar profiles reveals some detailed characteristics and complex structure of diurnal cold air pools in this region. The study will be extended to other cases and compared with stable processes in urban basins (Doran et al. 2002).

7. REFERENCES

Astling, E.G., 1998: Investigation of the boundary layer in a mountain valley with a lower atmospheric profiler. Preprints *8th Conference on Mountain Meteorology,* Amer. Meteorol. Soc., Flagstaff, AZ, 386-389.

Clements, C.B., C.D. Whiteman, and J.D. Horel, 2000: Observations of a cold air pool in a remote mountain basin. Preprints *14th Symposium on Boundary Layer and Turbulence*, Aspen, CO, Amer. Meteorol. Soc., 457-460.

Doran, C., J. Fast, and J. Horel, 2002: The VTMX 2000 campaign. *Bull. Amer. Meteorol. Soc.*

Horel, J., and Coauthors, 2002: Mesonet: Cooperative mesonets in the western United States. *Bull. Amer. Meteorol. Soc.*, **83**, 211-225.

Eaton, F.D., S.A. McLaughlin, et al., 1995: A new frequency modulated-continuous wave radar for studying planetary boundary layer morphology. *Radio Science*, **30**, 75-88.

Metzger, M.M., J.C. Klewicki, K.L. Bradshaw, and R. Sadr, 2001: Scaling the near-wall axial turbulent stress in the zero pressure gradient boundary layer. *Phys. Fluids*, **13**, 1819.

Rife, D.L., T.T. Warner, F. Chen, and E.G. Astling, 2002: Mechanisms for diurnal boundary layer circulations in the Great Basin Desert. *Mon. Wea. Rev.*, **130**, 921-938.

Smith, R.B., 1989: Hydrostatic flow over mountains. *Adv. Geophys.*, Academic Press, **31**, 1-41.

Smith, R.B., and Coauthors, 1997: Local and remote effects of mountains on weather. Research needs and oppor-tunities. *Bull. Amer. Meteorol. Soc.,* **78**, 877-892.

Whiteman, C.D., S Zhong, W.J. Shaw, J.M. Hubbe, and X. Bian, 2001: Cold pools in the Columbia Basin. *Wea. Forecasting,* **16**, 432-447.